

# Characteristics-Based Schemes for the Hyperbolic Heat Conduction Equations

Brian J. McCartin

Applied Mathematics, Kettering University  
1700 West University Avenue, Flint, MI 48504-4898 USA  
bmccarti@kettering.edu

## Abstract

In [1], we derived and studied three fourth-order accurate characteristics-based schemes with unit Courant number for the hyperbolic heat conduction equations. Herein, we extend these schemes to Courant number less than unity although they are then only second-order accurate. The dissipative and dispersive properties of these extended schemes are compared to those of their continuum counterpart. These three schemes then are exercised on a smooth numerical example for which the exact solution is known.

**Mathematics Subject Classification:** 35L45, 65M06, 65M25

**Keywords:** hyperbolic heat conduction equations, numerical method of characteristics, dispersion and dissipation analysis, higher-order accuracy

## 1 Introduction

In [1], we studied the application of the numerical method of characteristics [2] with unit Courant number to fourth-order accurate approximation of the Cauchy problem for the source-free hyperbolic heat conduction equations [3]:

$$\frac{\partial \theta}{\partial t} + \frac{\partial q}{\partial x} = 0; \quad -\infty < x < \infty, \quad t > 0, \quad (1)$$

$$\tau \frac{\partial q}{\partial t} + q + \frac{\partial \theta}{\partial x} = 0; \quad -\infty < x < \infty, \quad t > 0, \quad (2)$$

subject to the initial conditions

$$\theta(x, 0) = \phi(x), \quad q(x, 0) = \psi(x); \quad -\infty < x < \infty. \quad (3)$$

In the above,  $\theta(x, t)$  is the temperature,  $q(x, t)$  is the heat flux, and  $\tau$  is the relaxation time. Equation (1) expresses the first law of thermodynamics (conservation of thermal energy) while Equation (2) embodies the Maxwell-Cattaneo law of heat conduction (modified Fourier's law).

Eliminating  $q$  from Equations (1) and (2) results in the (hyperbolic) damped wave equation

$$\frac{1}{a^2} \frac{\partial^2 \theta}{\partial t^2} + \frac{\partial \theta}{\partial t} = \frac{\partial^2 \theta}{\partial x^2}; \quad -\infty < x < \infty, \quad t > 0, \quad (4)$$

where  $a = \tau^{-1/2}$  is the thermal propagation speed. Observe that when  $\tau = 0$  (Fourier law of heat conduction), the wave speed is infinite and Equation (4) reduces to the (parabolic) diffusion equation.

In some emerging technologies such as fast-pulsed laser heating of materials, transient heat transfer at low cryogenic temperatures, and microwave heating with very high frequencies, the wave nature of thermal phenomena must be properly taken into account. Wiggert [4] first applied the numerical method of characteristics to the hyperbolic heat conduction equations.

Equations (1-2) are said to be in nonconservative form. Multiplication of both equations by the integrating factor  $e^{t/\tau}$  yields the conservative form of the hyperbolic heat conduction equations:

$$\frac{\partial \theta}{\partial t} + \frac{\partial q}{\partial x} = 0, \quad (5)$$

$$\frac{\partial [qe^{t/\tau}]}{\partial t} + \frac{\partial [(\theta/\tau)e^{t/\tau}]}{\partial x} = 0. \quad (6)$$

Equations (5-6) reveal that  $\theta$  and  $qe^{t/\tau}$  are conserved quantities with fluxes  $q$  and  $(\theta/\tau)e^{t/\tau}$ , respectively.

In the numerical method of characteristics, the hyperbolic heat conduction equations are transformed to characteristic form prior to discretization. Introduction of the characteristic coordinates (see Figure 1),

$$\zeta = t + \tau^{1/2}x; \quad \eta = t - \tau^{1/2}x, \quad (7)$$

transforms Equations (1-2) to the nonconservative characteristic form:

$$\frac{\partial \theta}{\partial \zeta} + \tau^{1/2} \left( \frac{\partial q}{\partial \zeta} + \frac{q}{2\tau} \right) = 0, \quad (8)$$

$$\frac{\partial \theta}{\partial \eta} - \tau^{1/2} \left( \frac{\partial q}{\partial \eta} + \frac{q}{2\tau} \right) = 0. \quad (9)$$

Likewise, Equations (5-6) transform to the conservative characteristic form:

$$e^{\zeta/2\tau} \frac{\partial \theta}{\partial \zeta} + \tau^{1/2} \frac{\partial [qe^{\zeta/2\tau}]}{\partial \zeta} = 0, \quad (10)$$

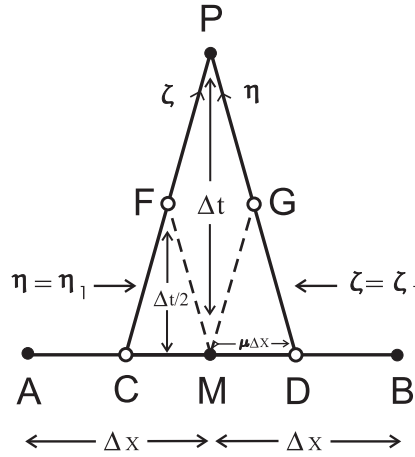


Figure 1: Stencil for Characteristics-Based Schemes

$$e^{\eta/2\tau} \frac{\partial \theta}{\partial \eta} - \tau^{1/2} \frac{\partial [qe^{\eta/2\tau}]}{\partial \eta} = 0. \tag{11}$$

In characteristic form, both the nonconservative and conservative forms of the hyperbolic heat conduction equations become ordinary differential equations along the characteristic lines with constant  $\zeta$  and  $\eta$ . Moreover, when the Courant number  $\mu = \tau^{-1/2} \Delta t / \Delta x$  equals one, the characteristic lines pass through the computational grid and either of the characteristic forms may be numerically integrated along the characteristics to yield nonconservative and conservative numerical schemes. Otherwise, additional interpolation on  $[A, B]$  is required. In accordance with the C-F-L condition [5], the restriction  $\mu \leq 1$  is necessary for stability.

## 2 Continuous Dispersion Relation

In [6], Roe and Arora make a convincing case that a comparison of the dispersive and dissipative properties of the hyperbolic heat conduction equations to those of their numerical approximations provides an important tool for assessing the suitability of the latter. So that we may perform such a comparison in later sections, we next summarize their continuous analysis of the dispersive and dissipative properties of the hyperbolic heat conduction equations.

By seeking Fourier mode solutions of Equations (1-2) of the form of a multiple of  $e^{i(\omega t - \xi x)}$ , we immediately arrive at the complex dispersion relation

$$\tau \omega^2 - \xi^2 - i \cdot \omega = 0, \tag{12}$$

where (real)  $\xi$  is a wave number and (complex)  $\omega$  may be written as  $\omega = \omega_R + i \cdot \omega_I$  with  $\omega_R$  an angular frequency and  $\omega_I$  a damping parameter.

The complex dispersion relation, Equation (12) may be broken into real and imaginary parts thereby yielding the pair of equations

$$\omega_R \cdot (1 - 2\tau\omega_I) = 0, \quad (13)$$

$$\omega_R^2 = \omega_I^2 + \frac{\xi^2 - \omega_I}{\tau}. \quad (14)$$

If  $\omega_R \neq 0$  then Equation (13) implies that

$$\omega_I = \frac{1}{2\tau} \quad (15)$$

and Equation (14) implies that

$$\omega_R = \pm \sqrt{\frac{\xi^2}{\tau} - \frac{1}{4\tau^2}}. \quad (16)$$

Defining the wave speed  $a(\xi) = \omega_R/\xi$  for  $\xi \neq 0$ , we have

$$a(\xi) = \pm \tau^{-1/2} \cdot \sqrt{1 - \frac{1}{4\tau\xi^2}}. \quad (17)$$

For high wave numbers,  $a(\xi)$  approaches the characteristic speed  $\tau^{-1/2}$  (frozen wave speed). For lower wave numbers,  $a(\xi)$  decreases, reaching zero when  $\xi = \frac{1}{2}\tau^{-1/2}$  (vanishing equilibrium wave speed). All waves with wave numbers in the range  $[\frac{1}{2}\tau^{-1/2}, \infty]$  are damped as  $e^{-t/2\tau}$ .

For wave numbers less than  $\frac{1}{2}\tau^{-1/2}$ ,  $\omega_R = 0$  and the waves do not propagate. After the relaxation time  $t = \tau$ , they are damped by  $e^{-\omega_I\tau}$  where

$$\omega_I\tau = \frac{1 \mp \sqrt{1 - 4\xi^2\tau}}{2}. \quad (18)$$

In Figure 2, the above dispersion analysis is summarized graphically. In the top graph, the nondimensional wave speed,  $\hat{a} = \tau^{1/2}a$  is plotted against the nondimensional wave number  $\hat{\xi} = \tau^{1/2}\xi$ . In the bottom graph, the damping rate  $e^{-\omega_I\tau}$  is plotted against the nondimensional wave number  $\hat{\xi} = \tau^{1/2}\xi$ .

Beginning at the wave number of zero, we have two stationary modes, one with a damping rate of 1 and the other with a damping rate of  $e^{-1}$ . As the wave number increases, these two damping rates begin to monotonically approach  $e^{-1/2}$ . At the nondimensional wave number of one-half, these two modes coalesce and thereafter bifurcate into two waves propagating in opposite directions with identical speeds and constant damping rate  $e^{-1/2}$ . The magnitude of the nondimensional wave speeds increase monotonically, approaching one in the limit of infinite wave number.

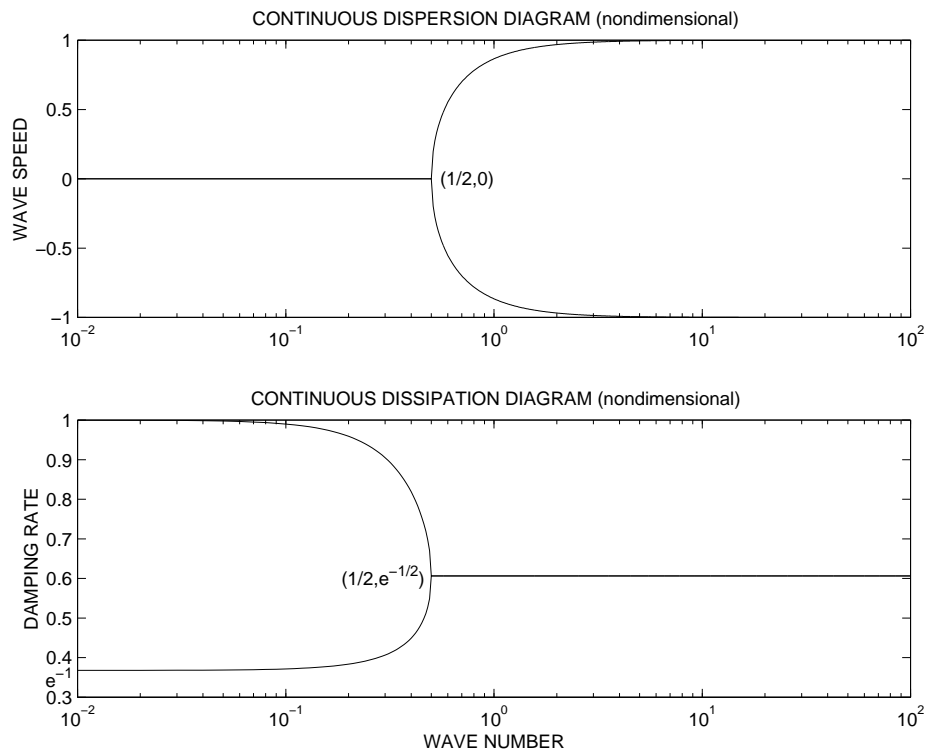


Figure 2: Continuous Dispersion/Dissipation Diagrams

### 3 Characteristics-Based Schemes

There is the following analytical solution to the Cauchy problem for the hyperbolic heat conduction equations (see Figure 1):

$$\theta_P = e^{-k} \cdot \frac{\theta_C + \theta_D}{2} + \frac{\tau^{1/2}}{2} \cdot \int_C^D \left( \frac{\Omega}{\tau} - \Omega_t \right) \cdot \theta \, dx - \frac{\tau^{1/2}}{2} \cdot \int_C^D \Omega \cdot q_x \, dx, \quad (19)$$

$$q_P = e^{-k} \cdot \frac{q_C + q_D}{2} + \frac{\tau^{1/2}}{2} \cdot \int_C^D \Omega_t \cdot q \, dx - \frac{\tau^{-1/2}}{2} \cdot \int_C^D \Omega \cdot \theta_x \, dx, \quad (20)$$

where  $\Omega$  is the Riemann function for this initial value problem [7, pp. 108-110]. Since these analytical expressions reveal that the exact solution at point  $P$  depends upon the values of  $\theta$  and  $q$  along the entire interval  $[C, D]$ , we will be exclusively concerned with coupled schemes of the following form which include information at the point  $M$ :

$$\theta_P = R_\theta(k) \cdot \frac{\theta_A + \theta_B}{2} + S_\theta(k) \cdot \frac{\tau^{1/2}}{2} \cdot (q_A - q_B) + T_\theta(k) \cdot (\theta_A - 2\theta_M + \theta_B), \quad (21)$$

$$q_P = R_q(k) \cdot \frac{q_A + q_B}{2} + S_q(k) \cdot \frac{\tau^{-1/2}}{2} \cdot (\theta_A - \theta_B) + T_q(k) \cdot (q_A - 2q_M + q_B), \quad (22)$$

where the stiffness parameter,  $k$ , is given by

$$k = \frac{1}{2} \cdot \frac{\Delta t}{\tau} = \frac{\mu}{2} \cdot \frac{\Delta x}{\tau^{1/2}}, \quad (23)$$

and the coefficients  $R_\theta, S_\theta, T_\theta, R_q, S_q, T_q$  determine the particular coupled scheme.

Equations (21) and (22) may be recast as

$$\theta_P = U(k) \cdot \frac{\theta_A + \theta_B}{2} + \frac{\tau^{1/2}}{2} \cdot X(k) \cdot (q_A - q_B) + V(k) \cdot \theta_M, \quad (24)$$

$$q_P = Z(k) \cdot \frac{q_A + q_B}{2} + \frac{\tau^{-1/2}}{2} \cdot Y(k) \cdot (\theta_A - \theta_B) + W(k) \cdot q_M, \quad (25)$$

where  $X = S_\theta, Y = S_q, Z = R_q + 2T_q, U = R_\theta + 2T_\theta, V = -2T_\theta, W = -2T_q$ .

Seeking Fourier mode solutions of Equations (24-25) in the form of  $(\theta, q) = e^{i(\omega \cdot n \Delta t - \xi \cdot j \Delta x)}(\hat{\theta}, \hat{q})$  [8], we require nonzero solutions to the homogeneous system

$$\begin{bmatrix} e^{i\omega \Delta t} - U \cos(\xi \Delta x) - V & -i\tau^{1/2} X \sin(\xi \Delta x) \\ -i\tau^{-1/2} Y \sin(\xi \Delta x) & e^{i\omega \Delta t} - Z \cos(\xi \Delta x) - W \end{bmatrix} \begin{bmatrix} \hat{\theta} \\ \hat{q} \end{bmatrix} = \begin{bmatrix} 0 \\ 0 \end{bmatrix}. \quad (26)$$

Setting the determinant of the coefficient matrix to zero, we immediately arrive at the complex dispersion relation for coupled schemes

$$e^{i\omega \Delta t} = \frac{1}{2} \cdot [B \pm \sqrt{B^2 - 4C}], \quad (27)$$

where

$$B := V + W + (U + Z) \cdot \cos(\xi \Delta x), \quad (28)$$

$$C := (UZ - XY) \cdot \cos^2(\xi \Delta x) + (UW + VZ) \cdot \cos(\xi \Delta x) + (XY + VW). \quad (29)$$

In the above, (real)  $\xi$  is a wave number and (complex)  $\omega$  may be written as  $\omega = \omega_R + i \cdot \omega_I$  with  $\omega_R$  an angular frequency and  $\omega_I$  a damping parameter. Denoting the complex amplification factor [5], Equation (27), by  $c^\pm$ , we have

$$\omega_R \Delta t = \text{Arg}(c) \quad (-\pi < \text{Arg}(\cdot) \leq \pi), \quad -\omega_I \Delta t = \ln |c^\pm|. \quad (30)$$

Before proceeding, let us make an important observation concerning the computation of the nondimensional wave speed  $\tau^{1/2} \cdot a$ . If  $|\omega_R \Delta t| > \xi \Delta x$  then  $|\omega_R / \xi| > \Delta x / \Delta t$ , i.e. the Fourier mode

$$[e^{-\omega_I \Delta t}]^n \cdot e^{i(\omega_R \cdot n \Delta t - \xi \cdot j \Delta x)} \quad (31)$$

travels faster than the grid speed. While acceptable mathematically, this interpretation violates physical causality and as such is not viable.

Instead, when  $|\omega_R \Delta t| > \pi/2$ , we rewrite Equation (31) as

$$[-e^{-\omega_I \Delta t}]^n \cdot e^{i(n \cdot (\omega_R \Delta t \pm \pi) - j \cdot \xi \Delta x)}. \tag{32}$$

Thus, we then reinterpret the Fourier mode as traveling with wave speed

$$\tau^{1/2} \cdot a^\pm = \begin{cases} \tau^{1/2} \cdot \frac{\omega_R^\pm}{\xi}, & \text{if } |\omega_R \Delta t| < \pi/2, \\ \tau^{1/2} \cdot \frac{\omega_R^\pm}{\xi} \mp \frac{\pi}{\xi \Delta x}, & \text{if } |\omega_R \Delta t| \geq \pi/2, \end{cases} \tag{33}$$

and possessing a damping rate

$$r = \begin{cases} e^{-\omega_I \tau}, & \text{if } |\omega_R \Delta t| < \pi/2, \\ -e^{-\omega_I \tau}, & \text{if } |\omega_R \Delta t| \geq \pi/2. \end{cases} \tag{34}$$

Note that for a negatively damped mode of the discretization, the amplitude of the wave not only decays but also oscillates in sign at successive time steps. There is no corresponding behavior exhibited by the original partial differential equations. Consequently, a thorough discrete dispersion/dissipation analysis requires that the distinction be made between positively and negatively damped modes.

Furthermore, the use of Equation (34) will produce a discontinuity in our plots of damping rate. This discontinuity is essential if physical causality is to be enforced. Using Equation (33) produces no corresponding discontinuity in wave speed. See [1] for an alternative perspective on defining wave speed.

With reference to Figure 1, we place the origin of coordinates at  $P(0, 0)$  so that we have  $A(-\Delta x, -\Delta t)$ ,  $M(0, -\Delta t)$ ,  $B(\Delta x, -\Delta t)$ ,  $C(-\mu \Delta x, 0)$ ,  $D(\mu \Delta x, 0)$ ,  $F(-\mu \Delta x/2, -\Delta t/2)$ ,  $G(\mu \Delta x/2, -\Delta t/2)$ . We then integrate Equations (10) and (11) by parts along the characteristics  $CP$  and  $DP$ , respectively, to obtain

$$(\theta_P - \theta_C e^{-2k}) + \tau^{1/2}(q_P - q_C e^{-2k}) = \frac{1}{\tau} \int_{CP} \theta(t) e^{t/\tau} dt, \tag{35}$$

$$(\theta_P - \theta_D e^{-2k}) - \tau^{1/2}(q_P - q_D e^{-2k}) = \frac{1}{\tau} \int_{DP} \theta(t) e^{t/\tau} dt. \tag{36}$$

Adding Equation (36) to Equation (35) and solving for  $\theta_P$  yields

$$\theta_P = e^{-2k} \left[ \frac{\theta_C + \theta_D}{2} + \frac{\tau^{1/2}}{2} (q_C - q_D) \right] + \frac{1}{2} \left[ \frac{1}{\tau} \int_{CP} \theta(t) e^{t/\tau} dt + \frac{1}{\tau} \int_{DP} \theta(t) e^{t/\tau} dt \right], \tag{37}$$

while subtracting Equation (36) from Equation (35) and solving for  $q_P$  yields

$$q_P = e^{-2k} \left[ \frac{q_C + q_D}{2} + \frac{\tau^{-1/2}}{2} (\theta_C - \theta_D) \right] + \frac{\tau^{-1/2}}{2} \left[ \frac{1}{\tau} \int_{CP} \theta(t) e^{t/\tau} dt - \frac{1}{\tau} \int_{DP} \theta(t) e^{t/\tau} dt \right]. \tag{38}$$

Equations (37) and (38) are exact. Below, we will obtain higher-order accurate schemes by numerically approximating the integrals which appear above [10].

In what follows, we will also require approximations to  $(\theta_C, q_C)$  and  $(\theta_D, q_D)$ . For this purpose, we employ parabolic approximations to  $(\theta, q)$  on  $[A, B]$ . Specifically, using the Newton form with centers located at  $x_A$  and  $x_M$  [10]:

$$\theta_{AB} = \theta_A + \frac{\theta_M - \theta_A}{\Delta x} \cdot (x - x_A) + \frac{\theta_B - 2\theta_M + \theta_A}{2(\Delta x)^2} \cdot (x - x_A)(x - x_M), \quad (39)$$

$$q_{AB} = \theta_A + \frac{q_M - q_A}{\Delta x} \cdot (x - x_A) + \frac{q_B - 2q_M + q_A}{2(\Delta x)^2} \cdot (x - x_A)(x - x_M). \quad (40)$$

Consequently,

$$\theta_C \approx \theta_A + (1 - \mu) \cdot (\theta_M - \theta_A) + \frac{\mu(\mu - 1)}{2} \cdot (\theta_B - 2\theta_M + \theta_A), \quad (41)$$

$$q_C \approx q_A + (1 - \mu) \cdot (q_M - q_A) + \frac{\mu(\mu - 1)}{2} \cdot (q_B - 2q_M + q_A), \quad (42)$$

$$\theta_D \approx \theta_A + (1 + \mu) \cdot (\theta_M - \theta_A) + \frac{\mu(\mu + 1)}{2} \cdot (\theta_B - 2\theta_M + \theta_A), \quad (43)$$

$$q_D \approx q_A + (1 + \mu) \cdot (q_M - q_A) + \frac{\mu(\mu + 1)}{2} \cdot (q_B - 2q_M + q_A). \quad (44)$$

Furthermore, differentiation of Equations (39) and (40) provide the requisite approximations to the following spatial derivatives of  $\theta$  and  $q$ :

$$(\theta_x)_C \approx \mu \cdot \frac{2(\theta_M - \theta_A) + (1 - 2\mu)(\theta_B - 2\theta_M + \theta_A)}{4k\tau^{1/2}}, \quad (45)$$

$$(q_x)_C \approx \mu \cdot \frac{2(q_M - q_A) + (1 - 2\mu)(q_B - 2q_M + q_A)}{4k\tau^{1/2}}, \quad (46)$$

$$(\theta_x)_M \approx \mu \cdot \frac{\theta_B - \theta_A}{4k\tau^{1/2}}; \quad (q_x)_M \approx \mu \cdot \frac{q_B - q_A}{4k\tau^{1/2}}, \quad (47)$$

$$(\theta_x)_D \approx \mu \cdot \frac{2(\theta_M - \theta_A) + (1 + 2\mu)(\theta_B - 2\theta_M + \theta_A)}{4k\tau^{1/2}}, \quad (48)$$

$$(q_x)_D \approx \mu \cdot \frac{2(q_M - q_A) + (1 + 2\mu)(q_B - 2q_M + q_A)}{4k\tau^{1/2}}, \quad (49)$$

$$(\theta_{xx})_C \approx \mu^2 \cdot \frac{\theta_B - 2\theta_M + \theta_A}{4k^2\tau} \approx (\theta_{xx})_D, \quad (50)$$

$$(q_{xx})_C \approx \mu^2 \cdot \frac{q_B - 2q_M + q_A}{4k^2\tau} \approx (q_{xx})_D, \quad (51)$$

where we have invoked the identity  $\Delta x = 2k\tau^{1/2}/\mu$ .

### 3.1 Fractional Step Scheme (FS)

We commence by assuming that the temperature varies quadratically along the characteristic  $CP$

$$\theta_{CP}(t) = \theta_P + \left( \frac{3\theta_P - 4\theta_F + \theta_C}{2k} \right) \cdot \left( \frac{t}{\tau} \right) + \left( \frac{\theta_C - 2\theta_F + \theta_P}{2k^2} \right) \cdot \left( \frac{t}{\tau} \right)^2, \quad (52)$$

as well as along the characteristic  $DP$

$$\theta_{DP}(t) = \theta_P + \left( \frac{3\theta_P - 4\theta_G + \theta_D}{2k} \right) \cdot \left( \frac{t}{\tau} \right) + \left( \frac{\theta_D - 2\theta_G + \theta_P}{2k^2} \right) \cdot \left( \frac{t}{\tau} \right)^2. \quad (53)$$

Thus,

$$\begin{aligned} \frac{1}{\tau} \int_{CP} \theta(t)e^{t/\tau} dt + \frac{1}{\tau} \int_{DP} \theta(t)e^{t/\tau} dt &= S_0 \cdot 2\theta_P \\ &+ S_1 \cdot \frac{6\theta_P - 4(\theta_F + \theta_G) + \theta_C + \theta_D}{2k} \\ &+ S_2 \cdot \frac{\theta_C + \theta_D - 2(\theta_F + \theta_G) + 2\theta_P}{2k^2}, \end{aligned} \quad (54)$$

$$\begin{aligned} \frac{1}{\tau} \int_{CP} \theta(t)e^{t/\tau} dt - \frac{1}{\tau} \int_{DP} \theta(t)e^{t/\tau} dt &= S_1 \cdot \frac{4(\theta_G - \theta_F) + \theta_C - \theta_D}{2k} \\ &+ S_2 \cdot \frac{\theta_C - \theta_D + 2(\theta_G - \theta_F)}{2k^2}, \end{aligned} \quad (55)$$

where

$$S_n := \frac{1}{\tau^{n+1}} \int_{-\Delta t}^0 t^n e^{t/\tau} dt \quad (56)$$

(see Appendix C).

In order for such a scheme to be second-order accurate, we require first-order accurate approximations to  $\theta_F$  and  $\theta_G$ . We obtain such first-order accurate approximations by taking an intermediate fractional time-step to estimate  $\theta_F$  and  $\theta_G$ .

By suitably modifying Equation (37) for a time-step of  $\Delta t/2$ , we obtain

$$\theta_F = e^{-k} \left[ \frac{\theta_C + \theta_M}{2} + \frac{\tau^{1/2}}{2} (q_C - q_M) \right] + \frac{e^k}{2} \left[ \frac{1}{\tau} \int_{CF} \theta(t)e^{t/\tau} dt + \frac{1}{\tau} \int_{MF} \theta(t)e^{t/\tau} dt \right], \quad (57)$$

$$\theta_G = e^{-k} \left[ \frac{\theta_M + \theta_D}{2} + \frac{\tau^{1/2}}{2} (q_M - q_D) \right] + \frac{e^k}{2} \left[ \frac{1}{\tau} \int_{MG} \theta(t)e^{t/\tau} dt + \frac{1}{\tau} \int_{DG} \theta(t)e^{t/\tau} dt \right]. \quad (58)$$

We next describe the computational procedure for  $\theta_F$  and obtain the corresponding expression for  $\theta_G$  via the substitutions  $F \leftarrow G, C \leftarrow M, M \leftarrow D$ .

Along the characteristic  $CF$ , we make the quadratic approximation

$$\begin{aligned} \theta_{CF}(t) = 4\theta_F - 3\theta_C - 2k\tau\theta'_C &+ \left( \frac{4\theta_F - 4\theta_C - 3k\tau\theta'_C}{k} \right) \cdot \left( \frac{t}{\tau} \right) \\ &+ \left( \frac{\theta_F - \theta_C - k\tau\theta'_C}{k^2} \right) \cdot \left( \frac{t}{\tau} \right)^2, \end{aligned} \tag{59}$$

while along the characteristic  $MF$ , we make the quadratic approximation

$$\begin{aligned} \theta_{MF}(t) = 4\theta_F - 3\theta_M - 2k\tau\theta'_M &+ \left( \frac{4\theta_F - 4\theta_M - 3k\tau\theta'_M}{k} \right) \cdot \left( \frac{t}{\tau} \right) \\ &+ \left( \frac{\theta_F - \theta_M - k\tau\theta'_M}{k^2} \right) \cdot \left( \frac{t}{\tau} \right)^2. \end{aligned} \tag{60}$$

In the above,

$$\theta'_C = (-q_x + \tau^{-1/2}\theta_x)_C; \theta'_M = (-q_x - \tau^{-1/2}\theta_x)_M. \tag{61}$$

Substitution of Equations (59) and (60) into Equation (57) followed by solution for  $\theta_F$  yields

$$\begin{aligned} \theta_F = [k^2\tau^{1/2}e^{-2k} \cdot (q_C - q_M) &+ (k^2e^{-2k} - 3k^2S_{0,1} - 4kS_{1,1} - S_{2,1}) \cdot (\theta_C + \theta_M) \\ &- (2k^3\tau S_{0,1} + 3k^2\tau S_{1,1} + k\tau S_{2,1}) \cdot (\theta'_C + \theta'_M)] \\ &/ [2(k^2e^{-2k} - 3k^2S_{0,1} - 4kS_{1,1} - S_{2,1})], \end{aligned} \tag{62}$$

where

$$S_{n,1} := \frac{1}{\tau^{n+1}} \int_{-\Delta t}^{-\Delta t/2} t^n e^{t/\tau} dt \tag{63}$$

(see Appendix C).

The corresponding expression for  $\theta_G$ , derivable from Equation (58), is

$$\begin{aligned} \theta_G = [k^2\tau^{1/2}e^{-2k} \cdot (q_M - q_D) &+ (k^2e^{-2k} - 3k^2S_{0,1} - 4kS_{1,1} - S_{2,1}) \cdot (\theta_M + \theta_D) \\ &- (2k^3\tau S_{0,1} + 3k^2\tau S_{1,1} + k\tau S_{2,1}) \cdot (\theta'_M + \theta'_D)] \\ &/ [2(k^2e^{-2k} - 3k^2S_{0,1} - 4kS_{1,1} - S_{2,1})], \end{aligned} \tag{64}$$

where

$$\theta'_M = (-q_x + \tau^{-1/2}\theta_x)_M; \theta'_D = (-q_x - \tau^{-1/2}\theta_x)_D. \tag{65}$$

Substitution of Equations (62) and (64) into Equations (54) and (55) and subsequent substitution into Equations (37) and (38), while also utilizing Equations (41-49), yield the Fractional Step scheme (FS):

$$R_\theta(k) = 1, \tag{66}$$

$$S_\theta(k) = \mu \cdot \frac{2k^2 e^{-2k} [k - 1 + e^{-k}] + [k - 1 + (k + 1)e^{-2k}] [k - 2 + (k^2 + k + 2)e^{-k}]}{[(3k - 2) + (k + 2)e^{-2k}] [(k - 1) + e^{-k}]}, \tag{67}$$

$$T_\theta(k) = -\frac{1}{2} + \mu^2 \cdot \frac{k(1 - e^{-k}) [k - 1 + (k + 1)e^{-2k}] + [k - 1 + e^{-k}] [2 - k - (3k + 2)e^{-2k}]}{2[(3k - 2) + (k + 2)e^{-2k}] [(k - 1) + e^{-k}]}, \tag{68}$$

$$R_q(k) = e^{-2k}, \tag{69}$$

$$S_q(k) = \mu \cdot \frac{1 - e^{-2k}}{2k}, \tag{70}$$

$$T_q(k) = \frac{\mu^2 - 1}{2} \cdot e^{-2k} + \mu^2 \cdot \frac{[k - 1 + (k + 1)e^{-2k}] [k - 2 + (k^2 + k + 2)e^{-k}]}{4k^2 [(k - 1) + e^{-k}]}. \tag{71}$$

### 3.1.1 Order of Accuracy

**Lemma 1** *For Equations (66-71):*

$$\begin{aligned} R_\theta(k) &= 1, \\ S_\theta(k) &= \mu - \mu k + \frac{2\mu}{3} k^2 - \frac{\mu}{3} k^3 + \frac{43\mu}{270} k^4 + \dots, \\ T_\theta(k) &= \frac{\mu^2 - 1}{2} - \frac{\mu^2}{3} k + \frac{\mu^2}{6} k^2 - \frac{43\mu^2}{540} k^3 + \dots, \\ R_q(k) &= 1 - 2k + 2k^2 - \frac{4}{3} k^3 + \frac{2}{3} k^4 - \frac{4}{15} k^5 + \dots, \\ S_q(k) &= \mu - \mu k + \frac{2\mu}{3} k^2 - \frac{\mu}{3} k^3 + \frac{2\mu}{15} k^4 + \dots, \\ T_q(k) &= \frac{\mu^2 - 1}{2} + \frac{3 - 2\mu^2}{3} k + \frac{\mu^2 - 2}{2} k^2 + \frac{30 - 11\mu^2}{45} k^3 + \dots. \end{aligned}$$

These facts imply our main result.

**Theorem 1** *The local discretization/truncation error (LTE) for the FS scheme, Equations (66-71), is  $O(k^3)$  if  $\mu < 1$  and is  $O(k^5)$  if  $\mu = 1$ .*

**Proof:** Simply apply the Order of Accuracy Theorem (Appendix B). The local discretization/truncation error is [9, p. 77]:

$$\begin{aligned} LTE_M^\theta &= \left[ \frac{4}{3} \left( \frac{1}{\mu^2} - 1 \right) \tau^2 q_{xxx} \right]_M \cdot k^3 \\ &+ \left[ \frac{2}{3} \left( 1 - \frac{1}{\mu^2} \right) \tau^2 \theta_{xxxx} + \frac{4}{3} \left( 1 - \frac{1}{\mu^2} \right) \tau^2 q_{xxx} \right]_M \cdot k^4 \\ &+ \left[ \frac{4}{15} \left( \frac{1}{\mu^4} - 1 \right) \tau^3 q_{xxxxx} + \left( \frac{20 - 24\mu^2}{45\mu^2} \right) \tau^2 \theta_{xxxx} + \left( \frac{40 - 36\mu^2}{45\mu^2} \right) \tau^2 q_{xxx} \right. \\ &\quad \left. + \left( \frac{43\mu - 36}{135} \right) \tau \theta_{xx} + \frac{7}{135} \tau q_x \right]_M \cdot k^5, \end{aligned}$$

$$\begin{aligned} LTE_M^q &= \left[ \frac{4}{3} \left( \frac{1}{\mu^2} - 1 \right) \tau \theta_{xxx} \right]_M \cdot k^3 \\ &+ \left[ \frac{2}{3} \left( 1 - \frac{1}{\mu^2} \right) \tau^2 q_{xxxx} + \frac{4}{3} \left( 1 - \frac{1}{\mu^2} \right) \tau \theta_{xxx} \right]_M \cdot k^4 \\ &+ \left[ \frac{4}{15} \left( \frac{1}{\mu^4} - 1 \right) \tau^2 \theta_{xxxxx} + \left( \frac{8}{9\mu^2} - \frac{4}{5} \right) \tau^2 q_{xxxx} + \left( \frac{8}{9\mu^2} - \frac{4}{5} \right) \tau \theta_{xxx} \right. \\ &\quad \left. - \frac{4}{45} \tau q_{xx} \right]_M \cdot k^5, \end{aligned}$$

which, for  $\mu = 1$ , reduces to:

$$\begin{aligned} LTE_M^\theta &= \frac{4\tau}{45} \cdot \left[ -\tau \theta_{xxxx} + \tau q_{xxx} + \frac{7}{12} \theta_{xx} + \frac{7}{12} q_x \right]_M \cdot k^5, \\ LTE_M^q &= \frac{4\tau}{45} \cdot \left[ \tau q_{xxxx} + \theta_{xxx} - q_{xx} \right]_M \cdot k^5. \quad \square \end{aligned}$$

The order of accuracy of the FS scheme follows immediately.

**Corollary 1** *The FS scheme, Equations (66-71), is second-order accurate for  $\mu < 1$  and is fourth-order accurate for  $\mu = 1$ .*

**Proof:** This follows by applying Theorem 2.4 of [9, p. 80] to Theorem 1.  $\square$

### 3.1.2 Dispersive and Dissipative Properties

Figures 3-4 provide a graphical summary of the dispersive and dissipative properties of the FS scheme with  $\mu = .9$  for  $k = 0.25, 0.50, 0.75, 1.00, 2.00$  and  $5.00$ . In these plots, the solid curves represent the exact values derived from the continuous dispersion relation, Equation (12), while the dotted curves derive from the discrete dispersion relation, Equation (27). Figure 3 displays the nondimensional wave speed,  $\tau^{1/2}a$ , and Figure 4 displays the damping rate,  $\pm e^{-\omega_I \tau}$ , for nondimensional wave numbers in the range  $0 < \hat{\xi} = \tau^{1/2} \xi \leq \hat{\xi}_{max} = \frac{\mu\pi}{2k}$ . Since the magnitude of the damping rate is bounded by unity, the FS scheme is stable for  $\mu \leq 1$ .

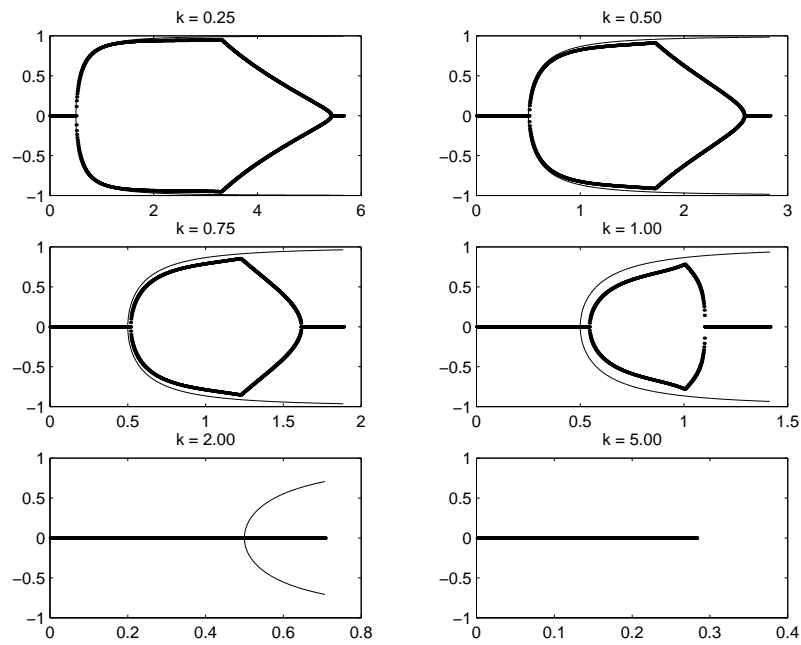


Figure 3: Wave Speed - FS Scheme ( $\mu = .9$ )

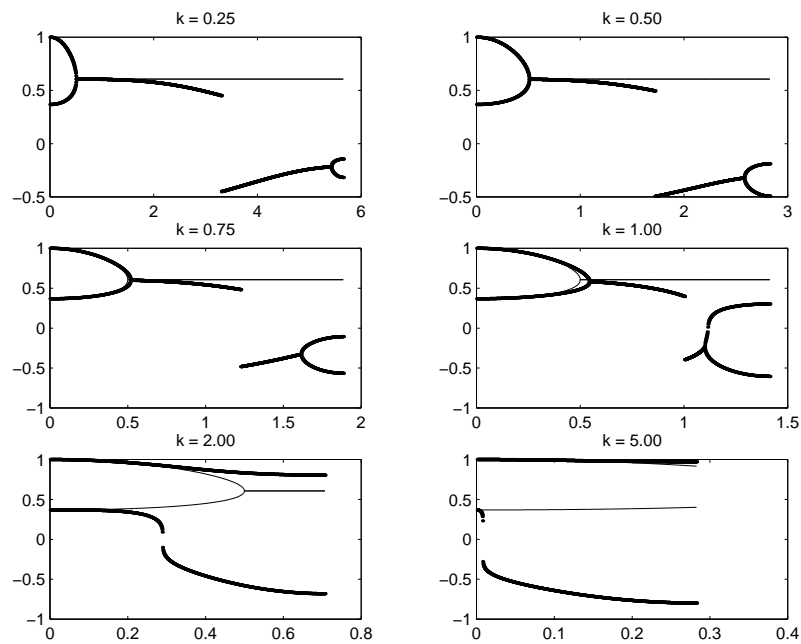


Figure 4: Damping Rate - FS Scheme ( $\mu = .9$ )

### 3.2 Hermite-Bessel Scheme (HB)

We next develop another fourth-order accurate scheme that does not rely upon a fractional time-step. Instead, we employ cubic Hermite-Bessel interpolation [10] to proceed directly from one time level to the next.

Specifically, along the characteristic  $CP$ , we make the cubic approximation

$$\begin{aligned} \theta_{CP}(t) = \theta_P &+ \left( \frac{-3(\theta_C - \theta_P) - 4k\tau\theta'_C - 2k^2\tau^2\theta''_C}{2k} \right) \cdot \left( \frac{t}{\tau} \right) \\ &+ \left( \frac{-3(\theta_C - \theta_P) - 6k\tau\theta'_C - 4k^2\tau^2\theta''_C}{4k^2} \right) \cdot \left( \frac{t}{\tau} \right)^2 \\ &+ \left( \frac{-(\theta_C - \theta_P) - 2k\tau\theta'_C - 2k^2\tau^2\theta''_C}{8k^3} \right) \cdot \left( \frac{t}{\tau} \right)^3, \end{aligned} \tag{72}$$

while, along the characteristic  $DP$ , we make the cubic approximation

$$\begin{aligned} \theta_{DP}(t) = \theta_P &+ \left( \frac{-3(\theta_D - \theta_P) - 4k\tau\theta'_D - 2k^2\tau^2\theta''_D}{2k} \right) \cdot \left( \frac{t}{\tau} \right) \\ &+ \left( \frac{-3(\theta_D - \theta_P) - 6k\tau\theta'_D - 4k^2\tau^2\theta''_D}{4k^2} \right) \cdot \left( \frac{t}{\tau} \right)^2 \\ &+ \left( \frac{-(\theta_D - \theta_P) - 2k\tau\theta'_D - 2k^2\tau^2\theta''_D}{8k^3} \right) \cdot \left( \frac{t}{\tau} \right)^3. \end{aligned} \tag{73}$$

Thus,

$$\begin{aligned} \frac{1}{\tau} \int_{CP} \theta(t)e^{t/\tau} dt &+ \frac{1}{\tau} \int_{DP} \theta(t)e^{t/\tau} dt = S_0 \cdot 2\theta_P \\ &- S_1 \cdot \frac{3(\theta_C - 2\theta_P + \theta_D) + 4k\tau(\theta'_C + \theta'_D) + 2k^2\tau^2(\theta''_C + \theta''_D)}{2k} \\ &- S_2 \cdot \frac{3(\theta_C - 2\theta_P + \theta_D) + 6k\tau(\theta'_C + \theta'_D) + 4k^2\tau^2(\theta''_C + \theta''_D)}{4k^2} \\ &- S_3 \cdot \frac{(\theta_C - 2\theta_P + \theta_D) + 2k\tau(\theta'_C + \theta'_D) + 2k^2\tau^2(\theta''_C + \theta''_D)}{8k^3}, \end{aligned} \tag{74}$$

$$\begin{aligned} \frac{1}{\tau} \int_{CP} \theta(t)e^{t/\tau} dt &- \frac{1}{\tau} \int_{DP} \theta(t)e^{t/\tau} dt = \\ &- S_1 \cdot \frac{3(\theta_C - \theta_D) + 4k\tau(\theta'_C - \theta'_D) + 2k^2\tau^2(\theta''_C - \theta''_D)}{2k} \\ &- S_2 \cdot \frac{3(\theta_C - \theta_D) + 6k\tau(\theta'_C - \theta'_D) + 4k^2\tau^2(\theta''_C - \theta''_D)}{4k^2} \\ &- S_3 \cdot \frac{(\theta_C - \theta_D) + 2k\tau(\theta'_C - \theta'_D) + 2k^2\tau^2(\theta''_C - \theta''_D)}{8k^3} \end{aligned} \tag{75}$$

In the above,

$$\theta'_C = (-q_x + \tau^{-1/2}\theta_x)_C; \theta''_C = (\tau^{-1}q_x - 2\tau^{-1/2}q_{xx} + 2\tau^{-1}\theta_{xx})_C, \tag{76}$$

$$\theta'_D = (-q_x - \tau^{-1/2}\theta_x)_D; \theta''_D = (\tau^{-1}q_x + 2\tau^{-1/2}q_{xx} + 2\tau^{-1}\theta_{xx})_D. \tag{77}$$

Substitution of Equations (76-77) into Equations (74-75) and subsequent substitution into Equations (37-38), while also utilizing Equations (41-51), yield the Hermite-Bessel scheme (HB):

$$R_\theta(k) = 1, \tag{78}$$

$$S_\theta(k) = \mu \cdot \frac{(2k^3 - 8k^2 + 9k - 3) + (-4k^3 - 4k^2 - 3k + 3)e^{-2k}}{3[(-2k^2 + 2k - 1) + e^{-2k}]}, \tag{79}$$

$$T_\theta(k) = -\frac{1}{2} + \mu^2 \cdot \frac{(-4k^2 + 4k - 6) + (8k^2 + 8k + 6)e^{-2k}}{12[(-2k^2 + 2k - 1) + e^{-2k}]}, \tag{80}$$

$$R_q(k) = e^{-2k}, \tag{81}$$

$$S_q(k) = \mu \cdot \frac{1 - e^{-2k}}{2k}, \tag{82}$$

$$T_q(k) = -\frac{1}{2} \cdot e^{-2k} + \mu^2 \cdot \frac{(-2k^2 + 6k - 5) + (2k^2 + 4k + 5)e^{-2k}}{4k^2}. \tag{83}$$

### 3.2.1 Order of Accuracy

**Lemma 2** For Equations (78-83):

$$\begin{aligned} R_\theta(k) &= 1, \\ S_\theta(k) &= \mu - \mu k + \frac{2\mu}{3}k^2 - \frac{\mu}{3}k^3 + \frac{\mu}{10}k^4 + \dots, \\ T_\theta(k) &= \frac{\mu^2 - 1}{2} - \frac{\mu^2}{3}k + \frac{\mu^2}{6}k^2 - \frac{\mu^2}{20}k^3 + \dots, \\ R_q(k) &= 1 - 2k + 2k^2 - \frac{4}{3}k^3 + \frac{2}{3}k^4 - \frac{4}{15}k^5 + \dots, \\ S_q(k) &= \mu - \mu k + \frac{2\mu}{3}k^2 - \frac{\mu}{3}k^3 + \frac{2\mu}{15}k^4 + \dots, \\ T_q(k) &= \frac{\mu^2 - 1}{2} + \frac{3 - 2\mu^2}{3}k + \frac{\mu^2 - 2}{2}k^2 + \frac{2 - \mu^2}{3}k^3 + \dots \end{aligned}$$

These facts imply our main result.

**Theorem 2** *The local discretization/truncation error (LTE) for the HB scheme, Equations (78-83), is  $O(k^3)$  if  $\mu < 1$  and is  $O(k^5)$  if  $\mu = 1$ .*

**Proof:** Simply apply the Order of Accuracy Theorem (Appendix B). The local discretization/truncation error is [9, p. 77]:

$$\begin{aligned} LTE_M^\theta &= \left[ \frac{4}{3} \left( \frac{1}{\mu^2} - 1 \right) \tau^2 q_{xxx} \right]_M \cdot k^3 \\ &+ \left[ \frac{2}{3} \left( 1 - \frac{1}{\mu^2} \right) \tau^2 \theta_{xxxx} + \frac{4}{3} \left( 1 - \frac{1}{\mu^2} \right) \tau^2 q_{xxx} \right]_M \cdot k^4 \\ &+ \left[ \frac{4}{15} \left( \frac{1}{\mu^4} - 1 \right) \tau^3 q_{xxxxx} + \left( \frac{20 - 24\mu^2}{45\mu^2} \right) \tau^2 \theta_{xxxx} + \left( \frac{40 - 36\mu^2}{45\mu^2} \right) \tau^2 q_{xxx} \right. \\ &\quad \left. + \left( \frac{3\mu - 4}{15} \right) \tau \theta_{xx} - \frac{1}{15} \tau q_x \right]_M \cdot k^5, \end{aligned}$$

$$\begin{aligned} LTE_M^q &= \left[ \frac{4}{3} \left( \frac{1}{\mu^2} - 1 \right) \tau \theta_{xxx} \right]_M \cdot k^3 \\ &+ \left[ \frac{2}{3} \left( 1 - \frac{1}{\mu^2} \right) \tau^2 q_{xxxx} + \frac{4}{3} \left( 1 - \frac{1}{\mu^2} \right) \tau \theta_{xxx} \right]_M \cdot k^4 \\ &+ \left[ \frac{4}{15} \left( \frac{1}{\mu^4} - 1 \right) \tau^2 \theta_{xxxxx} + \left( \frac{8}{9\mu^2} - \frac{4}{5} \right) \tau^2 q_{xxxx} + \left( \frac{8}{9\mu^2} - \frac{4}{5} \right) \tau \theta_{xxx} \right. \\ &\quad \left. + \frac{4}{15} \tau q_x \right]_M \cdot k^5, \end{aligned}$$

which, for  $\mu = 1$ , reduces to:

$$LTE_M^\theta = \frac{4\tau}{45} \cdot \left[ -\tau \theta_{xxxx} + \tau q_{xxx} - \frac{3}{4} \theta_{xx} - \frac{3}{4} q_x \right]_M \cdot k^5,$$

$$LTE_M^q = \frac{4\tau}{45} \cdot \left[ \tau q_{xxxx} + \theta_{xxx} + 3q_x \right]_M \cdot k^5. \quad \square$$

The order of accuracy of the HB scheme follows immediately.

**Corollary 2** *The HB scheme, Equations (78-83), is second-order accurate for  $\mu < 1$  and is fourth-order accurate for  $\mu = 1$ .*

**Proof:** This follows by applying Theorem 2.4 of [9, p. 80] to Theorem 2.  $\square$

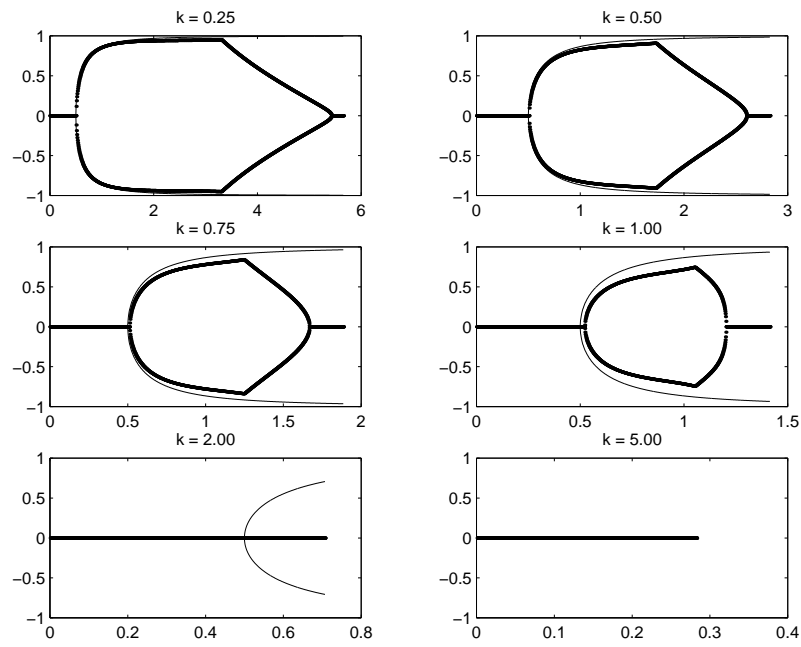


Figure 5: Wave Speed - HB Scheme ( $\mu = .9$ )

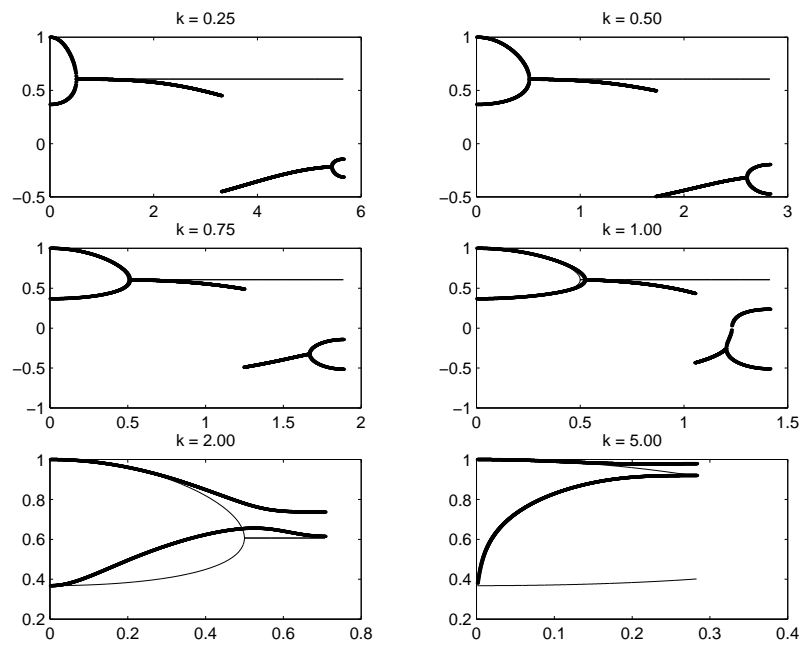


Figure 6: Damping Rate - HB Scheme ( $\mu = .9$ )

### 3.2.2 Dispersive and Dissipative Properties

Figures 5-6 provide a graphical summary of the dispersive and dissipative properties of the HB scheme with  $\mu = .9$  for  $k = 0.25, 0.50, 0.75, 1.00, 2.00$  and  $5.00$ . In these plots, the solid curves represent the exact values derived from the continuous dispersion relation, Equation (12), while the dotted curves derive from the discrete dispersion relation, Equation (27). Figure 5 displays the nondimensional wave speed,  $\tau^{1/2}a$ , and Figure 6 displays the damping rate,  $\pm e^{-\omega_I\tau}$ , for nondimensional wave numbers in the range  $0 < \hat{\xi} = \tau^{1/2}\xi \leq \hat{\xi}_{max} = \frac{\mu\pi}{2k}$ . Since the magnitude of the damping rate is bounded by unity, the HB scheme is stable for  $\mu \leq 1$ .

### 3.3 Hybrid Scheme (HYBRID)

The individual equations of the FS and HB schemes may be averaged to yield a scheme which is fourth-order accurate for  $\mu = 1$  with improved principal local truncation errors for  $\mu \leq 1$ . We thereby arrive at the Hybrid scheme (HYBRID):

$$R_\theta(k) = \frac{9}{16}R_\theta^{FS}(k) + \frac{7}{16}R_\theta^{HB}(k), \quad (84)$$

$$S_\theta(k) = \frac{9}{16}S_\theta^{FS}(k) + \frac{7}{16}S_\theta^{HB}(k), \quad (85)$$

$$T_\theta(k) = \frac{9}{16}T_\theta^{FS}(k) + \frac{7}{16}T_\theta^{HB}(k), \quad (86)$$

$$R_q(k) = \frac{3}{4}R_q^{FS}(k) + \frac{1}{4}R_q^{HB}(k), \quad (87)$$

$$S_q(k) = \frac{3}{4}S_q^{FS}(k) + \frac{1}{4}S_q^{HB}(k), \quad (88)$$

$$T_q(k) = \frac{3}{4}T_q^{FS}(k) + \frac{1}{4}T_q^{HB}(k). \quad (89)$$

#### 3.3.1 Order of Accuracy

**Lemma 3** For Equations (84-89):

$$\begin{aligned} R_\theta(k) &= 1, \\ S_\theta(k) &= \mu - \mu k + \frac{2\mu}{3}k^2 - \frac{\mu}{3}k^3 + \frac{2\mu}{15}k^4 + \dots, \\ T_\theta(k) &= \frac{\mu^2 - 1}{2} - \frac{\mu^2}{3}k + \frac{\mu^2}{6}k^2 - \frac{\mu^2}{15}k^3 + \dots, \\ R_q(k) &= 1 - 2k + 2k^2 - \frac{4}{3}k^3 + \frac{2}{3}k^4 - \frac{4}{15}k^5 + \dots, \end{aligned}$$

$$\begin{aligned}
 S_q(k) &= \mu - \mu k + \frac{2\mu}{3}k^2 - \frac{\mu}{3}k^3 + \frac{2\mu}{15}k^4 + \dots, \\
 T_q(k) &= \frac{\mu^2 - 1}{2} + \frac{3 - 2\mu^2}{3}k + \frac{\mu^2 - 2}{2}k^2 + \frac{10 - 4\mu^2}{15}k^3 + \dots.
 \end{aligned}$$

These facts imply our main result.

**Theorem 3** *The local discretization/truncation error (LTE) for the HYBRID scheme, Equations (84-89), is  $O(k^3)$  if  $\mu < 1$  and is  $O(k^5)$  if  $\mu = 1$ .*

**Proof:** Simply apply the Order of Accuracy Theorem (Appendix B). The local discretization/truncation error is [9, p. 77]:

$$\begin{aligned}
 LTE_M^\theta &= \left[ \frac{4}{3} \left( \frac{1}{\mu^2} - 1 \right) \tau^2 q_{xxx} \right]_M \cdot k^3 \\
 &+ \left[ \frac{2}{3} \left( 1 - \frac{1}{\mu^2} \right) \tau^2 \theta_{xxxx} + \frac{4}{3} \left( 1 - \frac{1}{\mu^2} \right) \tau^2 q_{xxx} \right]_M \cdot k^4 \\
 &+ \left[ \frac{4}{15} \left( \frac{1}{\mu^4} - 1 \right) \tau^3 q_{xxxxx} + \left( \frac{20 - 24\mu^2}{45\mu^2} \right) \tau^2 \theta_{xxxx} + \left( \frac{40 - 36\mu^2}{45\mu^2} \right) \tau^2 q_{xxx} \right. \\
 &\quad \left. + \frac{4}{15} (\mu - 1) \tau \theta_{xx} \right]_M \cdot k^5,
 \end{aligned}$$

$$\begin{aligned}
 LTE_M^q &= \left[ \frac{4}{3} \left( \frac{1}{\mu^2} - 1 \right) \tau \theta_{xxx} \right]_M \cdot k^3 \\
 &+ \left[ \frac{2}{3} \left( 1 - \frac{1}{\mu^2} \right) \tau^2 q_{xxxx} + \frac{4}{3} \left( 1 - \frac{1}{\mu^2} \right) \tau \theta_{xxx} \right]_M \cdot k^4 \\
 &+ \left[ \frac{4}{15} \left( \frac{1}{\mu^4} - 1 \right) \tau^2 \theta_{xxxxx} + \left( \frac{8}{9\mu^2} - \frac{4}{5} \right) \tau^2 q_{xxxx} + \left( \frac{8}{9\mu^2} - \frac{4}{5} \right) \tau \theta_{xxx} \right]_M \cdot k^5,
 \end{aligned}$$

which, for  $\mu = 1$ , reduces to:

$$LTE_M^\theta = \frac{4\tau}{45} \cdot [-\tau \theta_{xxxx} + \tau q_{xxx}]_M \cdot k^5,$$

$$LTE_M^q = \frac{4\tau}{45} \cdot [\tau q_{xxxx} + \theta_{xxx}]_M \cdot k^5. \quad \square$$

The order of accuracy of the HYBRID scheme follows immediately.

**Corollary 3** *The HYBRID scheme, Equations (84-89), is second-order accurate for  $\mu < 1$  and is fourth-order accurate for  $\mu = 1$ .*

**Proof:** This follows by applying Theorem 2.4 of [9, p. 80] to Theorem 3.  $\square$

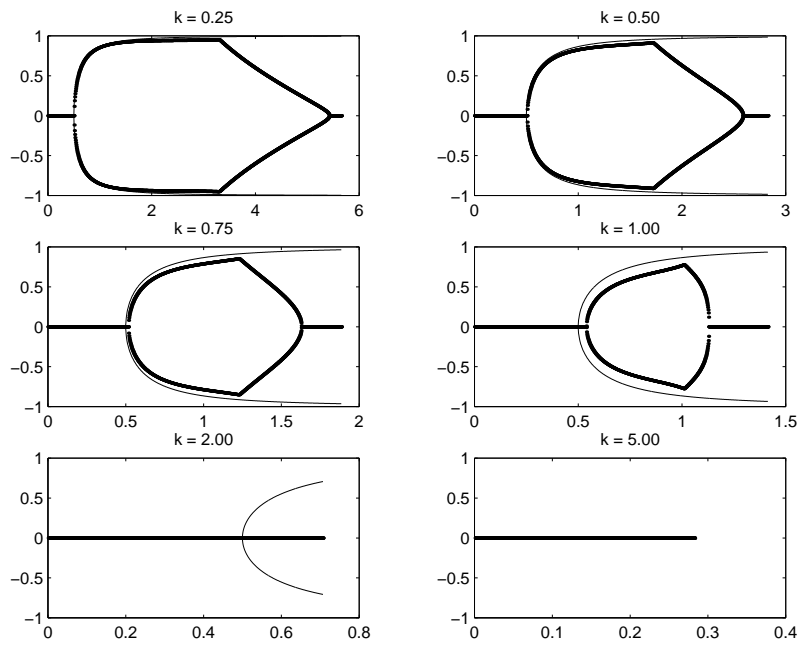


Figure 7: Wave Speed - HYBRID Scheme ( $\mu = .9$ )

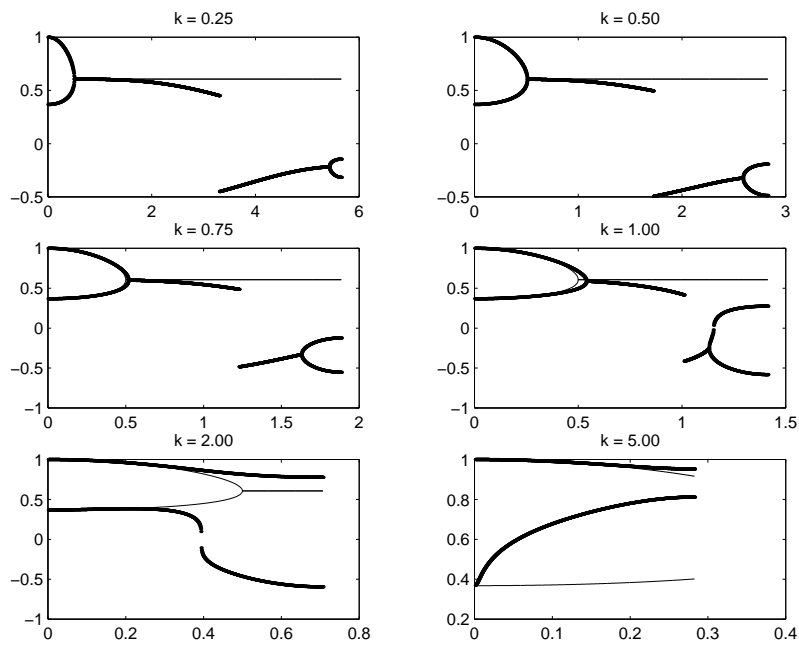


Figure 8: Damping Rate - HYBRID Scheme ( $\mu = .9$ )

### 3.3.2 Dispersive and Dissipative Properties

Figures 7-8 provide a graphical summary of the dispersive and dissipative properties of the HYBRID scheme with  $\mu = .9$  for  $k = 0.25, 0.50, 0.75, 1.00, 2.00$  and  $5.00$ . In these plots, the solid curves represent the exact values derived from the continuous dispersion relation, Equation (12), while the dotted curves derive from the discrete dispersion relation, Equation (27). Figure 7 displays the nondimensional wave speed,  $\tau^{1/2}a$ , and Figure 8 displays the damping rate,  $\pm e^{-\omega_I \tau}$ , for nondimensional wave numbers in the range  $0 < \hat{\xi} = \tau^{1/2}\xi \leq \hat{\xi}_{max} = \frac{\mu\pi}{2k}$ . Since the magnitude of the damping rate is bounded by unity, the HYBRID scheme is stable for  $\mu \leq 1$ .

## 4 Numerical Example

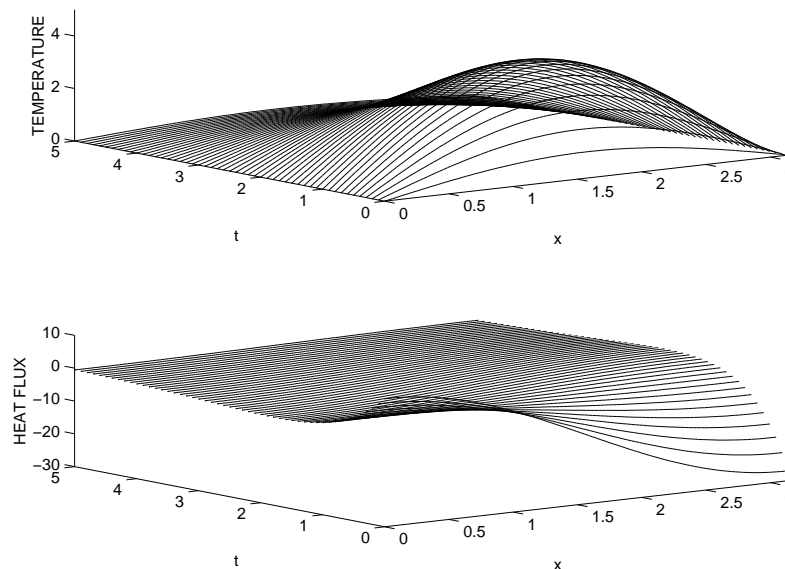


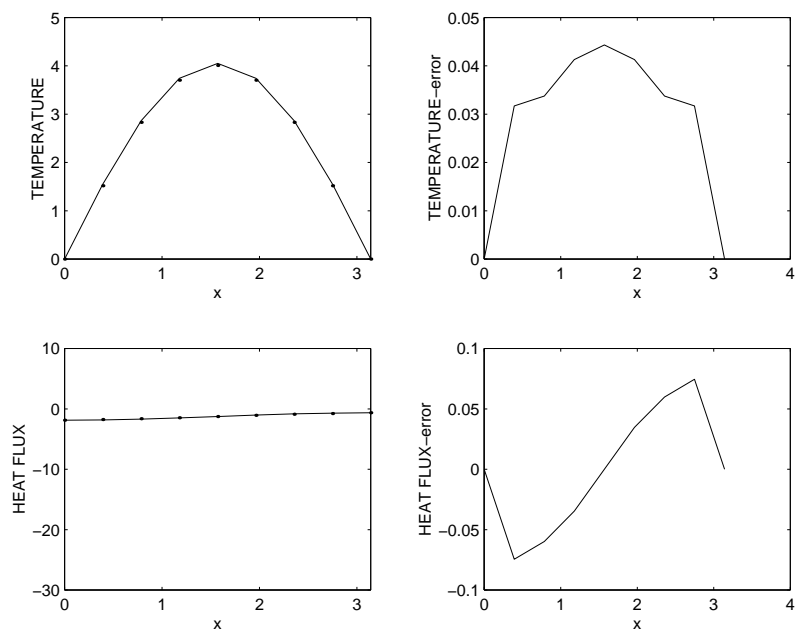
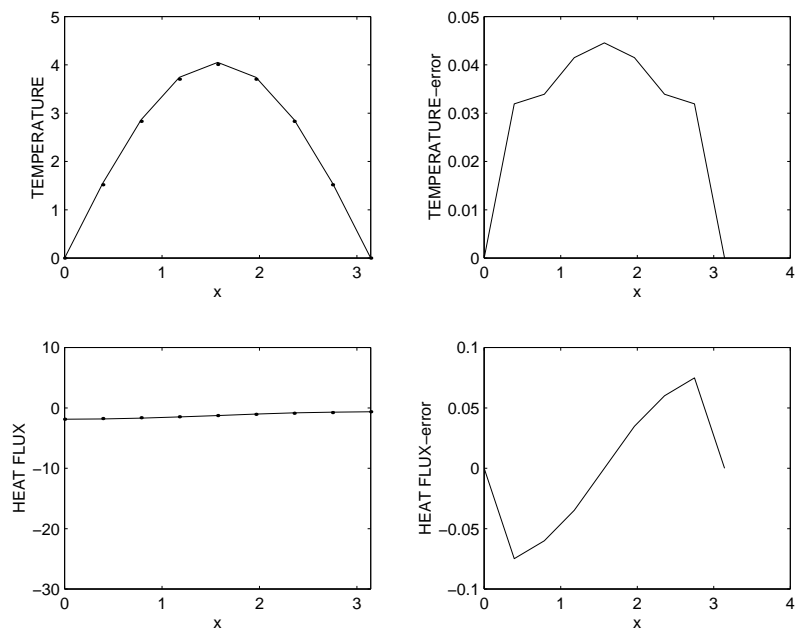
Figure 9: Exact Solution - Equations (90-91)

Consider the exact solution to the hyperbolic heat conduction equations [11]:

$$\theta(x, t) = \sin\left(\frac{x}{2\tau^{1/2}}\right) \cdot e^{-t/(2\tau)} \cdot \left(\alpha + \beta \cdot \frac{t}{2\tau}\right), \quad (90)$$

$$q(x, t) = \gamma \cdot e^{-t/\tau} - \tau^{-1/2} \cdot \cos\left(\frac{x}{2\tau^{1/2}}\right) \cdot e^{-t/(2\tau)} \cdot \left(\alpha - \beta + \beta \cdot \frac{t}{2\tau}\right). \quad (91)$$

This solution is on display in Figure 9 for  $\alpha = 1, \beta = 10, \gamma = -9$ , and  $\tau = 1/4$  on the interval  $0 \leq x \leq 2\pi \cdot \tau^{1/2}$ . The temperature profile at first rises

Figure 10: Numerical Approximation - FS Scheme ( $\mu = .5$ )Figure 11: Numerical Approximation - HB Scheme ( $\mu = .5$ )

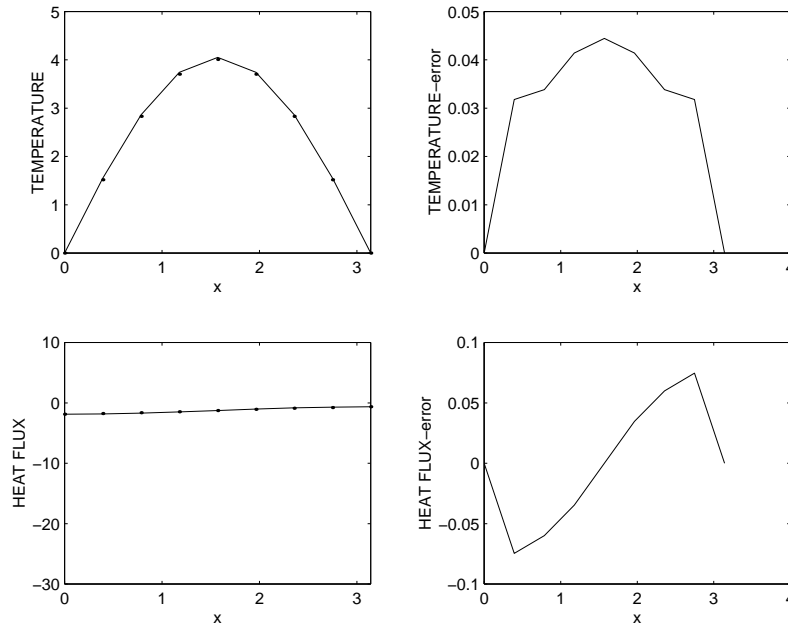


Figure 12: Numerical Approximation - HYBRID Scheme ( $\mu = .5$ )

to a maximum when  $t = 2(\beta - \alpha\tau^2)/(\beta\tau)$  before asymptotically approaching zero.

We next apply the FS, HB and HYBRID schemes to this problem. These numerical approximations with  $\mu = 1/2$  and  $\Delta x = \pi/8$  at the time when the temperature profile is cresting are displayed in Figures 10, 11 and 12, respectively. As might be expected for  $k = \pi/16$ , all three schemes provide comparable accuracy.

## 5 Conclusion

The benefits of higher-order accurate schemes for wave propagation problems are clearly presented in [12]. It might reasonably be expected that second-order accurate schemes which become fourth-order accurate for  $\mu = 1$  would inherit some of these same benefits for  $\mu < 1$ , especially when  $\mu \approx 1$ . Our dispersive/dissipative analysis and numerical results for the FS, HB and HYBRID schemes confirm this expectation. The HYBRID scheme possesses the additional advantage that, for  $\mu = 1$ , its principal local truncation errors (LTEs) coincide with those of the OPT scheme [6] and, for  $\mu < 1$ , the lowest order derivatives of  $q$  are absent from its LTEs. It should be noted that the stability limit for all three schemes is  $\mu_{max}(k) > 1$  but, for  $1 < \mu \leq \mu_{max}$ , they are only second-order accurate.

In closing, the preceding analysis has been confined to the pure initial value problem for the source-free hyperbolic heat conduction equations. In principle, coupled characteristics-based schemes may be extended to the initial-boundary value problem with a heat source. However, as discovered in [13], this considerably complicates the details and exposition, especially for higher-order accurate methods. Finally, extension of these higher-order accurate approximations to nonlinear hyperbolic heat transfer problems [14] is an open problem.

## 6 Acknowledgement

The author expresses his sincere gratitude to Mrs. Barbara A. McCartin for her dedicated assistance in the production of this paper.

## A Derivative Formulas

Successive differentiation and substitution of Equations (1) and (2) permits the exchange of temporal derivatives for spatial derivatives (assuming that the requisite derivatives exist and are continuous):

$$\theta_t = -q_x$$

$$\theta_{tt} = \tau^{-1} \cdot \theta_{xx} + \tau^{-1} \cdot q_x$$

$$\theta_{ttt} = -\tau^{-1} \cdot q_{xxx} - \tau^{-2} \cdot \theta_{xx} - \tau^{-2} \cdot q_x$$

$$\theta_{tttt} = \tau^{-2} \cdot \theta_{xxxx} + 2\tau^{-2} \cdot q_{xxx} + \tau^{-3} \cdot \theta_{xx} + \tau^{-3} \cdot q_x$$

$$\theta_{ttttt} = -\tau^{-2} \cdot q_{xxxxx} - 2\tau^{-3} \cdot \theta_{xxxx} - 3\tau^{-3} \cdot q_{xxx} - \tau^{-4} \cdot \theta_{xx} - \tau^{-4} \cdot q_x$$

$$q_t = -\tau^{-1} \cdot \theta_x - \tau^{-1} \cdot q$$

$$q_{tt} = \tau^{-1} \cdot q_{xx} + \tau^{-2} \cdot \theta_x + \tau^{-2} \cdot q$$

$$q_{ttt} = -\tau^{-2} \cdot \theta_{xxx} - 2\tau^{-2} \cdot q_{xx} - \tau^{-3} \cdot \theta_x - \tau^{-3} \cdot q$$

$$q_{tttt} = \tau^{-2} \cdot q_{xxxx} + 2\tau^{-3} \cdot \theta_{xxx} + 3\tau^{-3} \cdot q_{xx} + \tau^{-4} \cdot \theta_x + \tau^{-4} \cdot q$$

$$q_{ttttt} = -\tau^{-3} \cdot \theta_{xxxxx} - 3\tau^{-3} \cdot q_{xxxx} - 3\tau^{-4} \cdot \theta_{xxx} - 4\tau^{-4} \cdot q_{xx} - \tau^{-5} \cdot \theta_x - \tau^{-5} \cdot q$$

## B Order of Accuracy Conditions

We provide necessary and sufficient conditions for coupled characteristics-based schemes, Equations (21) and (22), to be first-, second-, third- and fourth-order accurate approximations to the hyperbolic heat conduction equations, Equations (1) and (2). For second- and fourth-order accurate schemes, we provide explicit expressions for their principal local truncation errors. It is shown that there exist accuracy barriers whereby, for  $\mu < 1$ , no such scheme can be third-order accurate and, for  $\mu = 1$ , no such scheme can be fifth-order accurate. In this sense, the FS, HB and HYBRID schemes developed above are optimal.

**Theorem 4 (Order of Accuracy)** *With reference to Equations (21) and (22), define*

$$R_\theta(k) = \sum_{n=0}^{\infty} A_n k^n, \quad S_\theta(k) = \sum_{n=0}^{\infty} B_n k^n, \quad T_\theta(k) = \sum_{n=0}^{\infty} C_n k^n,$$

and

$$R_q(k) = \sum_{n=0}^{\infty} a_n k^n, \quad S_q(k) = \sum_{n=0}^{\infty} b_n k^n, \quad T_q(k) = \sum_{n=0}^{\infty} c_n k^n.$$

Then, Equations (21) and (22) are

1. first-order accurate (consistent) if and only if  $A_0 = 1, A_1 = 0, B_0 = \mu; a_0 = 1, a_1 = -2, b_0 = 1,$
2. second-order accurate if and only if they are first-order accurate and  $A_2 = 0, B_1 = -\mu, C_0 = \frac{\mu^2-1}{2}; a_2 = 2, b_1 = -1, c_0 = \frac{\mu^2-1}{2},$
3. third-order accurate if and only if they are second-order accurate and  $\mu = 1, A_3 = 0, B_2 = \frac{2}{3}, C_1 = -\frac{1}{3}; a_3 = -\frac{4}{3}, b_2 = \frac{2}{3}, c_1 = \frac{1}{3},$
4. fourth-order accurate if and only if they are third-order accurate and  $A_4 = 0, B_3 = -\frac{1}{3}, C_2 = \frac{1}{6}; a_4 = \frac{2}{3}, b_3 = -\frac{1}{3}, c_2 = -\frac{1}{2}.$

If second-order accurate then the principal local truncation errors of Equations (21) and (22) are

$$\begin{aligned} LTE_M^\theta &= \left[ \frac{4}{3} \left( \frac{1}{\mu^2} - 1 \right) \tau^2 q_{xxx} - 4 \left( \frac{C_1}{\mu^2} + \frac{1}{3} \right) \tau \theta_{xx} + 2 \left( \frac{B_2}{\mu} + \frac{1}{3} \right) \tau q_x - A_3 \theta \right]_M \cdot k^3 \\ &+ \left[ \frac{2}{3} \left( 1 - \frac{1}{\mu^2} \right) \tau^2 \theta_{xxxx} + \frac{4}{3} \left( 1 - \frac{1}{\mu^2} \right) \tau^2 q_{xxx} + \left( \frac{2}{3} - \frac{4C_2}{\mu} \right) \tau \theta_{xx} \right. \\ &\quad \left. + 2 \left( \frac{B_3}{\mu} + \frac{1}{3} \right) \tau q_x - A_4 \theta \right]_M \cdot k^4 \\ &+ \left[ \frac{4}{15} \left( \frac{1}{\mu^4} - 1 \right) \tau^3 q_{xxxxx} + \left( \frac{20 - 24\mu^2}{45\mu^2} \right) \tau^2 \theta_{xxxx} + \left( \frac{40 - 36\mu^2}{45\mu^2} \right) \tau^2 q_{xxx} \right. \\ &\quad \left. - 4 \left( \frac{C_3}{\mu} + \frac{1}{15} \right) \tau \theta_{xx} + 2 \left( \frac{B_4}{\mu} - \frac{2}{15} \right) \tau q_x - A_5 \theta \right]_M \cdot k^5, \end{aligned}$$

$$\begin{aligned}
 LTE_M^q &= \left[ \frac{4}{3} \left( \frac{1}{\mu^2} - 1 \right) \tau \theta_{xxx} + 4 \left( \frac{1 - c_1}{\mu^2} - \frac{2}{3} \right) \tau q_{xx} + 2 \left( \frac{b_2}{\mu} - \frac{2}{3} \right) \theta_x \right. \\
 &\quad \left. - \left( a_3 + \frac{4}{3} \right) q \right]_M \cdot k^3 \\
 &+ \left[ \frac{2}{3} \left( 1 - \frac{1}{\mu^2} \right) \tau^2 q_{xxxx} + \frac{4}{3} \left( 1 - \frac{1}{\mu^2} \right) \tau \theta_{xxx} + 4 \left( \frac{1}{2} - \frac{1 + c_2}{\mu^2} \right) \tau q_{xx} \right. \\
 &\quad \left. + 2 \left( \frac{b_3}{\mu} + \frac{1}{3} \right) \theta_x + \left( \frac{2}{3} - a_4 \right) q \right]_M \cdot k^4 \\
 &+ \left[ \frac{4}{15} \left( \frac{1}{\mu^4} - 1 \right) \tau^2 \theta_{xxxxx} + \left( \frac{8}{9\mu^2} - \frac{4}{5} \right) \tau^2 q_{xxxx} + \left( \frac{8}{9\mu^2} - \frac{4}{5} \right) \tau \theta_{xxx} \right. \\
 &\quad \left. + \left( \frac{8}{3\mu^2} - \frac{4c_3}{\mu^2} - \frac{16}{15} \right) \tau q_{xx} + \left( \frac{2b_4}{\mu} - \frac{4}{15} \right) \theta_x - \left( a_5 + \frac{4}{15} \right) q \right]_M \cdot k^5,
 \end{aligned}$$

respectively. If  $\mu < 1$  then Equations (21) and (22) cannot be third-order accurate.

If fourth-order accurate then the principal local truncation errors of Equations (21) and (22) are

$$LTE_M^\theta = \frac{4\tau}{45} \cdot \left[ -\tau \theta_{xxxx} + \tau q_{xxx} - 45 \left( C_3 + \frac{1}{15} \right) \theta_{xx} + \frac{45}{2} \left( B_4 - \frac{2}{15} \right) q_x - \frac{45}{4\tau} A_5 \theta \right]_M \cdot k^5,$$

$$LTE_M^q = \frac{4\tau}{45} \cdot \left[ \tau q_{xxxx} + \theta_{xxx} - 45 \left( c_3 - \frac{2}{5} \right) q_{xx} + \frac{45}{2\tau} \left( b_4 - \frac{2}{15} \right) \theta_x - \frac{45}{4\tau} \left( a_5 + \frac{4}{15} \right) q \right]_M \cdot k^5,$$

respectively. Equations (21) and (22) cannot be fifth-order accurate. It is assumed that the initial data are sufficiently smooth so that all requisite derivatives exist and are continuous.

**Proof:** By Taylor’s Theorem,

$$\theta_P = \left[ \theta + 2\tau k \theta_t + 2\tau^2 k^2 \theta_{tt} + \frac{4}{3} \tau^3 k^3 \theta_{ttt} + \frac{2}{3} \tau^4 k^4 \theta_{tttt} + \frac{4}{15} \tau^5 k^5 \theta_{ttttt} \right]_M + O(k^6),$$

$$q_P = \left[ q + 2\tau k q_t + 2\tau^2 k^2 q_{tt} + \frac{4}{3} \tau^3 k^3 q_{ttt} + \frac{2}{3} \tau^4 k^4 q_{tttt} + \frac{4}{15} \tau^5 k^5 q_{ttttt} \right]_M + O(k^6).$$

Using the identities of Appendix A, these may be rewritten as

$$\begin{aligned}
 \theta_P &= \left[ \theta - 2\tau k q_x + 2\tau^2 k^2 (\tau^{-1} \theta_{xx} + \tau^{-1} q_x) \right. \\
 &\quad + \frac{4}{3} \tau^3 k^3 (-\tau^{-1} q_{xxx} - \tau^{-2} \theta_{xx} - \tau^{-2} q_x) \\
 &\quad + \frac{2}{3} \tau^4 k^4 (\tau^{-2} \theta_{xxxx} + 2\tau^{-2} q_{xxx} + \tau^{-3} \theta_{xx} + \tau^{-3} q_x) \\
 &\quad + \frac{4}{15} \tau^5 k^5 (-\tau^{-2} q_{xxxxx} - 2\tau^{-3} \theta_{xxxx} - 3\tau^{-3} q_{xxx} - \tau^{-4} \theta_{xx} - \tau^{-4} q_x) \left. \right]_M \\
 &\quad + O(k^6),
 \end{aligned}$$

$$\begin{aligned}
 q_P &= [q + 2\tau k(-\tau^{-1}\theta_x - \tau^{-1}q) + 2\tau^2 k^2(\tau^{-1}q_{xx} + \tau^{-2}\theta_x + \tau^{-2}q) \\
 &+ \frac{4}{3}\tau^3 k^3(-\tau^{-2}\theta_{xxx} - 2\tau^{-2}q_{xx} - \tau^{-3}\theta_x - \tau^{-3}q) \\
 &+ \frac{2}{3}\tau^4 k^4(\tau^{-2}q_{xxxx} + 2\tau^{-3}\theta_{xxx} + 3\tau^{-3}q_{xx} + \tau^{-4}\theta_x + \tau^{-4}q) \\
 &+ \frac{4}{15}\tau^5 k^5(-\tau^{-3}\theta_{xxxxx} - 3\tau^{-3}q_{xxxx} - 3\tau^{-4}\theta_{xxx} - 4\tau^{-4}q_{xx} - \tau^{-5}\theta_x - \tau^{-5}q)]_M \\
 &+ O(k^6).
 \end{aligned}$$

Also by Taylor's Theorem,

$$\frac{\theta_A + \theta_B}{2} = [\theta + \frac{2}{\mu^2}\tau k^2\theta_{xx} + \frac{2}{3\mu^4}\tau^2 k^4\theta_{xxxx}]_M + O(k^6),$$

$$\frac{\tau^{1/2}}{2} \cdot (q_A - q_B) = [-\frac{2}{\mu}\tau k q_x - \frac{4}{3\mu^3}\tau^2 k^3 q_{xxx} - \frac{4}{15\mu^5}\tau^3 k^5 q_{xxxxx}]_M + O(k^6),$$

$$\theta_A - 2\theta_M + \theta_B = [\frac{4}{\mu^2}\tau k^2\theta_{xx} + \frac{4}{3\mu^4}\tau^2 k^4\theta_{xxxx}]_M + O(k^6),$$

$$\frac{q_A + q_B}{2} = [q + \frac{2}{\mu^2}\tau k^2 q_{xx} + \frac{2}{3\mu^4}\tau^2 k^4 q_{xxxx}]_M + O(k^6),$$

$$\frac{\tau^{-1/2}}{2} \cdot (\theta_A - \theta_B) = [-\frac{2}{\mu}k\theta_x - \frac{4}{3\mu^3}\tau k^3\theta_{xxx} - \frac{4}{15\mu^5}\tau^2 k^5\theta_{xxxxx}]_M + O(k^6),$$

$$q_A - 2q_M + q_B = [\frac{4}{\mu^2}\tau k^2 q_{xx} + \frac{4}{3\mu^4}\tau^2 k^4 q_{xxxx}]_M + O(k^6).$$

Substitution of all of these Taylor series into Equations (21) and (22) and subsequent comparison of like powers of  $k$  directly establishes the theorem.  $\square$

### C Some Useful Integrals

$$S_{0,1} := \frac{1}{\tau} \int_{-\Delta t}^{-\Delta t/2} e^{t/\tau} dt = e^{-k} - e^{-2k}$$

$$S_{1,1} := \frac{1}{\tau^2} \int_{-\Delta t}^{-\Delta t/2} t e^{t/\tau} dt = -(1+k)e^{-k} + (1+2k)e^{-2k}$$

$$S_{2,1} := \frac{1}{\tau^3} \int_{-\Delta t}^{-\Delta t/2} t^2 e^{t/\tau} dt = (2+2k+k^2)e^{-k} + (-2-4k-4k^2)e^{-2k}$$

$$S_0 := \frac{1}{\tau} \int_{-\Delta t}^0 e^{t/\tau} dt = 1 - e^{-2k}$$

$$S_1 := \frac{1}{\tau^2} \int_{-\Delta t}^0 t e^{t/\tau} dt = -1 + (1 + 2k)e^{-2k}$$

$$S_2 := \frac{1}{\tau^3} \int_{-\Delta t}^0 t^2 e^{t/\tau} dt = 2 + (-2 - 4k - 4k^2)e^{-2k}$$

$$S_3 := \frac{1}{\tau^4} \int_{-\Delta t}^0 t^3 e^{t/\tau} dt = -6 + (6 + 12k + 12k^2 + 8k^3)e^{-2k}$$

## References

- [1] B. J. McCartin, Fourth-Order Accurate Simplified Coupled Characteristics- Based Schemes for the Hyperbolic Heat Conduction Equations, *Applied Mathematical Sciences*, Vol. 3, 2009, no. 10, 461-490.
- [2] M. B. Abbott, *An Introduction to the Method of Characteristics*, American Elsevier, New York, NY, 1966.
- [3] A. V. Luikov, *Analytical Heat Diffusion Theory*, Academic, New York, NY, 1968.
- [4] D. C. Wiggert, Analysis of Early-Time Transient Heat Conduction by Method of Characteristics, *ASME Journal of Heat Transfer*, 99 (1977), 35-40.
- [5] K. W. Morton and D. F. Mayers, *Numerical Solution of Partial Differential Equations*, Cambridge, 1994.
- [6] P. L. Roe and M. Arora, Characteristic-based schemes for dispersive waves I. The method of characteristics for smooth solutions, *Numerical Methods for Partial Differential Equations*, 9 (1993), 459-505.
- [7] P. D. Lax, *Partial Differential Equations*, Courant Institute of Mathematical Sciences, New York University, 1951.
- [8] J. W. Thomas, *Numerical Partial Differential Equations: Finite Difference Methods*, Springer, New York, NY, 1995.
- [9] P. Henrici, *Discrete Variable Methods in Ordinary Differential Equations*, Wiley, New York, NY, 1962.
- [10] S. D. Conte and C. de Boor, *Elementary Numerical Analysis: An Algorithmic Approach, Third Edition*, McGraw-Hill, New York, NY, 1980.
- [11] F. H. Miller, *Partial Differential Equations*, Wiley, New York, NY, 1941.
- [12] B. Gustafsson, *High Order Difference Methods for Time Dependent PDE*, Springer, New York, 2008.

- [13] B. J. McCartin and M. F. Causley, Angled Derivative Approximation of the Hyperbolic Heat Conduction Equations, *Applied Mathematics and Computation*, 182 (2006), 1581-1607.
- [14] H. Q. Yang, Characteristics-Based, High-Order Accurate and Nonoscillatory Numerical Method for Hyperbolic Heat Conduction, *Numerical Heat Transfer, Part B*, 18 (1990), 221-241.

**Received: January 2009**